

Hybrid algorithm for simulating the collimated transmittance of homogeneous stratified turbid media

Beatriz Morales Cruzado,^{1,4} José Alberto Delgado Atencio,³ Sergio Vázquez y Montiel,^{3,*} and Erick Sarmiento Gómez²

¹ Facultad de Ingeniería, Universidad Autónoma de San Luis Potosí, Álvaro Obregón 64, San Luis Potosí, S.L.P. Mexico

² Instituto de Física “Manuel Sandoval Vallarta”, Universidad Autónoma de San Luis Potosí, Álvaro Obregón 64, San Luis Potosí, S.L.P. Mexico

³ Universidad Politécnica de Tulancingo, División de Ingenierías, Tulancingo, Mexico

⁴ Consejo Nacional de Ciencia y Tecnología (CONACYT), Mexico

*sergiovazquez6969@gmail.com

<https://sites.google.com/site/betymoralescr/home/collimated>

Abstract: In this work we describe the development of a program that simulates the propagation of photons through refractive and reflecting optical components such as lenses, mirrors and stops that includes a biological tissue sample as the main issue to be investigated in order to get a simulated value of light distribution, in particular, of the unscattered light. The analysis of the photons that travel through the sample is based on the program Monte Carlo Multi-Layered with some modifications that consider a Gaussian beam as initial source of light. Position, directional cosines and weight of photons exiting the turbid media are used to propagate them through an optical system. As a mean of validation of the program, we selected a typical optical system for measurement of collimated transmittance. Therefore, several tests were carried out to find the optical system that gives the theoretical collimated transmittance at different values of the optical properties of the turbid media. Along this validation, the optimal experimental configuration is found. Using this results, a comparison between the simulated optimal configuration and the experimental set-up was done, by using a colloidal suspension as a turbid media.

©2015 Optical Society of America

OCIS codes: (170.0170) Medical optics and biotechnology; (170.6935) Tissue characterization; (170.3660) Light propagation in tissues; (220.3620) Lens system design.

References and links

1. S. A. Prah, M. J. C. van Gemert, and A. J. Welch, “Determining the optical properties of turbid media by using the adding-doubling method,” *Appl. Opt.* **32**(4), 559–568 (1993).
2. M. Hammer, A. Roggan, D. Schweitzer, and G. Müller, “Optical properties of ocular fundus tissues-an in vitro study using the double-integrating-sphere technique and inverse Monte Carlo simulation,” *Phys. Med. Biol.* **40**(6), 963–978 (1995).
3. B. Morales and S. Vázquez, “Obtención de los parámetros ópticos de la piel usando algoritmos genéticos y MCML,” *Rev. Mex. Fis.* **57**(4), 375–381 (2011).
4. B. Morales Cruzado, S. V. Y Montiel, and J. A. Atencio, “Genetic algorithms and MCML program for recovery of optical properties of homogeneous turbid media,” *Biomed. Opt. Express* **4**(3), 433–446 (2013).
5. A. M. Nilsson, C. Stureson, D. L. Liu, and S. Andersson-Engels, “Changes in spectral shape of tissue optical properties in conjunction with laser-induced thermotherapy,” *Appl. Opt.* **37**(7), 1256–1267 (1998).
6. A. M. Nilsson, G. W. Lucassen, W. Verkrusse, S. Andersson-Engels, and M. J. van Gemert, “Changes in optical properties of human whole blood in vitro due to slow heating,” *Photochem. Photobiol.* **65**(2), 366–373 (1997).

7. M. Friebel, A. Roggan, G. Müller, and M. Meinke, "Determination of optical properties of human blood in the spectral range 250 to 1100 nm using Monte Carlo simulations with hematocrit-dependent effective scattering phase functions," *J. Biomed. Opt.* **11**(3), 034021 (2006).
8. L. Wang and S. L. Jacques, "Error estimation of measuring total interaction coefficients of turbid media using collimated light transmission," *Phys. Med. Biol.* **39**(12), 2349–2354 (1994).
9. S. Avriillier, E. Tinet, and E. Delettre, "Monte Carlo simulation of collimated beam transmission through turbid media," *J. Phys.* **51**(22), 2521–2542 (1990).
10. L. Quan, Z. Changfang, and R. Nirmala, "Experimental validation of Monte Carlo modeling of fluorescence in tissues in the UV-visible spectrum," *J. Biomed. Opt.* **8**(2), 223–236 (2003).
11. C. Zhu and Q. Liu, "Numerical investigation of lens based setup for depth sensitive diffuse reflectance measurements in an epithelial cancer model," *Opt. Express* **20**(28), 29807–29822 (2012).
12. ZEMAX Development Corporation, ZEMAX Optical Design Program User's Guide (2003).
13. Lambda Research Corporation, TracePro 5.0 User's Manual (2009).
14. "http://www.scatlab.org", November 2011.
15. Lihong Wang and Steven L. Jacques, Monte Carlo Modeling of Light Transport in Multi-layered Tissues in Standard C (1998).
16. L. Wang, S. L. Jacques, and L. Zheng, "MCML- Monte Carlo modeling of light transport in multi-layered tissues," *Comput. Methods Programs Biomed.* **47**(2), 131–146 (1995).
17. W. J. Smith, *Modern Optical Engineering*, 4th ed. (SPIE PRESS, 2008).
18. W. T. Welford, *Aberration of Optical Systems* (Finite Ray tracing, 1991) Chap. 4.
19. H. C. van de Hulst, *Multiple Light Scattering* (Academic Press, New York, 1980), Vol. 1.
20. A. M. Nilsson, R. Berg, and S. Andersson-Engels, "Measurements of the optical properties of tissue in conjunction with photodynamic therapy," *Appl. Opt.* **34**(21), 4609–4619 (1995).
21. E. Alerstam, W. C. Lo, T. D. Han, J. Rose, S. Andersson-Engels, and L. Lilje, "Next-generation acceleration and code optimization for light transport in turbid media using GPUs," *Biomed. Opt. Express* **1**(2), 658–675 (2010).

1. Introduction

In biomedical optics focused on medical diagnosis, two main problems often arise, namely the forward and the inverse problem. In the forward problem from the knowledge of light source distribution, optical properties and geometry of the medium, the spatial distribution of light throughout the medium is predicted. On the other hand, for the inverse problem, the optical properties of the medium are determined from the knowledge of the light distribution and geometry of the medium. In both cases the use of mathematical models (deterministic or stochastic, etc.) that describe the transport of light in terms of optical properties and other parameters is of primary importance.

One possible way of solving the inverse problem is by making measurements of diffuse reflectance (R), diffuse transmittance (T) and collimated transmittance (T_c) in combination with an indirect interactive method such as Inverse Adding Doubling [1], Inverse Monte Carlo [2] or GA-MCML [3,4]. With three experimental measurements, the whole set of three optical parameters, scattering, absorption and anisotropy coefficients, can be recovered. The experimental measurements of diffuse reflectance and diffuse transmittance of a turbid sample can be easily obtained using a system of two integrating spheres [5–7]. In contrast, a "good measurement" of collimated transmittance, T_c , is often complicated to guarantee because even when it requires a minimal amount of instrumentation, the optimal configuration for its measurement depends on the optical properties of the sample under study [8]. A possible solution to this inconvenient could be to perform a "simulation" of collimated transmittance as guidance for experimental measurements.

A few examples of the use of Monte Carlo simulation of collimated transmittance can be found in the literature [9], but a detail study of the experimental problems regarding this measurement is missing. The Monte Carlo method has also been used in combination with optical components (fiber optics, lenses, etc.) by several research groups of the biomedical optics community [10, 11]. For example, Liu et al. [10] carried out MC simulations and experimental measurements for different configurations of fiber optic probes that were designed to detect diffuse reflectance and fluorescence of small tissue volumes of turbid media. Zhu and Liu in 2012 [11] reported on the Monte Carlo simulation of a non-contact diffuse reflectance optical experimental array that involved a lens in combination with an optical fiber. This simulation has some limitations, for instance, the lens is considered ideally

thin and without aberrations which in the case of the simulations performed could significantly modified the results. Both research works provide meaningful insights on how to consider the presence of optical components in a MC simulation of light-turbid media interaction but the computer codes employed are not publically available.

One alternative of simulation of T_c , is to consider the use of available commercial ray tracing program such as Zemax which offer a great variety of tools for designing, analyzing and optimizing simple and complex optical systems [12]. In spite of all this good features, Zemax in what concerns to biological systems, has some restrictions, for example, absorption cannot be taken into account without the use of user-designed scattering models, and photon propagation data, such as individual photon trajectories, cannot be accessible to the user, limiting the physical properties Zemax can quantify. On top of that, this program is not always reachable by all the researchers of the biomedical optics field due to the cost of its license. Another alternative is to use TracePro which allows the propagation of rays in a solid model without restrictions, the rays can be absorbed, reflected, refracted, scattered or diffracted [13], but in this program, as Zemax, the information at the output of the optical system does not match the parameters required for this type of application. Finally, we could consider simulating the light transport within tissues using ScatLab a program that bases its operation on Mie theory, especially the T-matrix formalism [14]. However, using this program to include optical components such as lenses, pinholes, etc., is a relatively difficult task.

In this work we propose a new solution to the outlined problem above, simulating an experimental arrangement designed to measure collimated transmittance by using a hybrid algorithm that combines the Monte Carlo Technique with the Ray Tracing method traditionally used in ray tracing algorithms. The system consists of an illumination source, a homogeneous slab of turbid medium representing a biological tissue sample and characterized by its optical parameters, some optical components such as lenses, pinholes and a detector. The hybrid computation program is presented and validated for the propagation of photons from a collimated light source with Gaussian distribution to a detector considering that between both elements there are sequentially a finite sample of turbid media and an array of pinholes. Light propagation within the turbid media is simulated using a modified version of the Monte Carlo code MCML developed by Lihong Wang and Steven Jacques [15,16]. In particular, the usefulness of the program to analyze the influence of certain parameters of the system in a typical configuration for measuring the collimated transmittance is investigated. Being based in a MCML algorithm, our program can be easily modified to fulfill user requirements. This algorithm is open source and free to use and can be downloaded from <https://sites.google.com/site/bettymoralescr/home/collimatedwhere> the user can also find useful information and the proper documentation for its use.

2. Materials and methods

2.1. Simulation of collimated transmittance

Monte Carlo Multi Layered program was used to simulate the propagation of photons within a turbid media [15, 16]. Original version of MCML requires an input file with the information of the optical properties of the sample to be simulated, such as thickness, refractive index, absorption, scattering coefficients and anisotropic factor. MCML produces an output file with important information, such as total reflectance, transmittance and absorption values, as well as absorption within the sample and radial and angular distribution of energy at the exit of the sample. However, for our purposes several modifications to the code were made.

MCML originally deals with a “pencil” beam, meaning that the simulated beam striking the first layer of the sample is dimensionless. To make more realistic the simulated situation, MCML program was modified in order to sample a Gaussian radial profile with a finite waist.

This was done by sampling a random variable χ between 0 and 1 and using

$$r = \omega \sqrt{\frac{-\ln(1-\chi)}{2}} \quad (1)$$

where r is the distance from the center to the entrance point of the photon. x and y positions of the photon were selected by randomly sampling another variable between 0 and 2π . Sampling Eq. (1) gives a Gaussian distribution of the form

$$S(r) = \frac{2}{\pi\omega^2} \exp\left(\frac{-2r^2}{\omega^2}\right) \quad (2)$$

where ω is the waist of the beam [17].

To facilitate the access to the information that MCML offers with respect to the position, direction and energy from each photon leaving the sample, we decide to include an instruction in the code to write orderly this information in a text file. The first three columns contain the coordinates (x, y, z) corresponding to the photon position at the last layer of the sample, in the following three columns the directional cosines are written (ux, uy, uz) that indicate the direction of the photon leaving the sample; finally, the seventh column indicates the weight of transmitted photon.

The next step in the development of the simulation set-up for calculating the collimated transmittance of a turbid sample is the propagation module. This was written in Visual Basic and requests, as the initial parameter, the total number of photons propagated through the optical set-up; this information is written in the MCML input file, and the program executes the MCML program. Next the file containing the coordinates and directional cosines of the photons at the exit of the turbid media is read and each photon is propagated in an optical system using standard ray tracing routines [18]. Each surface can be a refractive surface, such as a lens, or an obstacle surface, such as a pinhole. Information regarding the optical set-up can be read from an external text file, and must include typical information required for the ray propagation, such as refraction index of the surfaces, distance between consecutive surfaces, radius of curvature, or if the current surface is a refractive one or is an obstacle. The ray tracing module was tested against commercial available programs, such as Zemax, using a combination of a single lens and a pinhole, and finding no difference between them within numerical errors. A list in the right part of the program shows the curvatures, diameters and refractive indexes of the elements of the system, and a second list shows the positions and directional cosines of the first photon that propagates within the optical system. If a photon being propagated within the optical setup internally reflects in a refractive surface, do not touch a surface or strikes an obstacle, the photon is terminated and all its energy is lost. Finally, the program shows the value of collimated transmittance, which is calculated as the ratio between the weight, or energy, of the photons reaching the detector and the total energy of the initial photons. The combination of the MCML program and the Visual Basic environment will be referred as “photon propagation program in an optical-biological system”.

Figure 1 shows a schematic representation of the proposed algorithm for the calculation of the unscattered light propagating through an optical system. The number of photons used in the MCML simulation was 500,000 for $\mu_s < 100$, and 1,000,000 for $\mu_s > 100$ or when the expected value for the collimated transmittance falls below 1×10^{-5} . 25 simulations were carried out and the error bar was estimated from the standard deviation of all simulations. A complete set of simulations was performed in less than 1 hour in a 4.0 GHz personal computer.

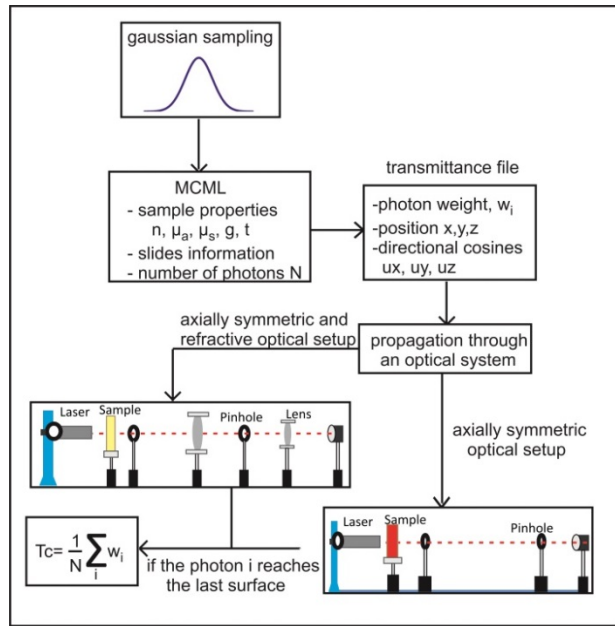


Fig. 1. Schematic representation of the “photon propagation program in an optical-biological system”.

2.2. Experimental measurements of collimated transmittance

Polystyrene plain microspheres of 1 μm diameter (standard deviation 0.1 μm , density 1.05 gr/cm^3) were purchased from Bangs Laboratories Inc. (Fishers, IN). The small standard deviation of commercial available plain microspheres makes it suitable for its use as an optical properties standard, as long as flocculation, sedimentation and evaporation are avoided. Water was Milli-Q water (nanopure-UV, USA; 18.3 M), thus avoiding the presence of ions that could produce flocculation. Sealed rectangular glass cells ($L = 0.1 \text{ cm}$) were supplied by Hellma. (USA). Starting sample was diluted several times to get a less scattering sample. Sample was re-dispersed prior each measurement and sedimentation was never observed in the measured samples. Scattering coefficients (μ_s) of each dilution were recovered by making reflectance and transmittance measurements with an integrating sphere (819C-SF-6, Newport, USA) at a wavelength of $\lambda = 514.5 \text{ nm}$ (Optotronics VD-III A) and using an intensity detector (ThorLabs DET10A) attached at north pole of the integrating sphere. The experimental set-up for total transmittance and reflectance measurements is shown in Fig. 2(A). Reflectance and transmittance were calculated as follows:

$$R = r_{std} \frac{R_r - R_0}{R_1 - R_0} \quad (3)$$

$$T = \frac{T_t - T_0}{T_1 - T_0} \quad (4)$$

where R_r is the power detected in reflectance mode with the sample placed in the exit port of the integrating sphere, R_0 is the correction factor for the stray light measured by detector with no sample and the entrance port uncovered, R_1 is power detected with a standard reflective surface at the exit port of integrating sphere, T_t is the power detected with the sample at entrance port in the integrating sphere in transmittance mode, T_0 is the correction factor measured with no sample and no light entering at the integrating sphere system, T_1 is the power detected with no sample and with a reflective surface at the exit port of integrating

sphere, r_{std} is the reflectance factor of the standard. The inversion technique used was inverse adding doubling (IAD) [1]. IAD is a general numerical solution of the radiative transport equation and consist of the following steps: (1) Guess a set of optical parameters, (2) calculate the reflection and transmission of the sample using the adding doubling method developed by van de Hulst [19], (3) compare the calculated values with the experimental measurements and (4) repeat the procedure until a match is made. IAD also takes into account several experimental uncertainty such as light lost out the edges and non-linear effects in integrating spheres measurements [1].

The experimental set-up for collimated transmittance measurements is shown in Fig. 2(B) and it mainly consists of two pinholes (diameter 2 mm) separated a distance d cm that are used to detect the light that travels parallel to the optical axis, *i.e.* the unscattered light. Collimated transmittance was measured as $T_c = I/I_0$ where I is the intensity sensed by the detector with the sample and I_0 is the intensity detected with the sample removed. In the case of a highly scattering sample, I measurements required a high laser power. In this case, detection of I_0 required a neutral filter (ThorLabs NE20A, ND = 2.0) to be placed before the sample to avoid detector saturation. Neutral filter density was taken into account in T_c calculations.

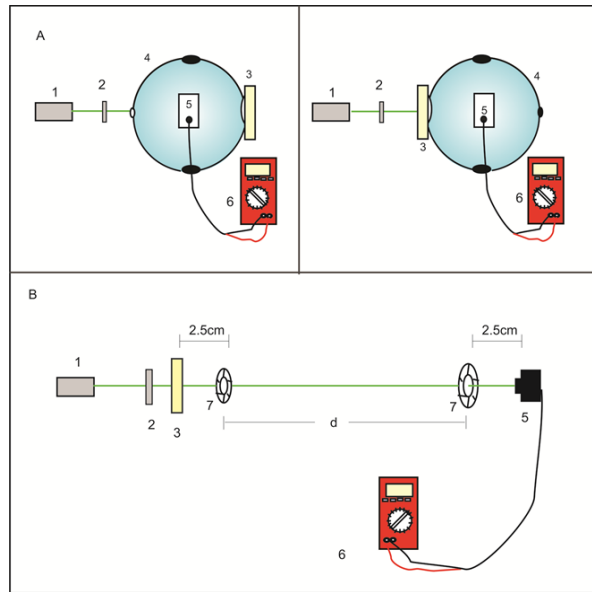


Fig. 2. A) On the left is shown the experimental set-up for reflectance measurements and on the right is outlined the experimental set-up for transmittance measurements. B) Experimental set-up for collimated transmittance measurements. The elements in the array are identified as follows: 1) Laser, 2) Neutral optical density filter, 3) sample 4) Integrating Sphere, 5) detector, 6) voltmeter and 7) pinholes

3. Results and discussion

Figure 3 shows the simulated intensity profile at the entrance of a turbid sample (black lines) and the intensity profile at the exit of the sample (red lines) at different value of the simulated beam waist coming from a MCML simulation. Both curves were normalized at maximum intensity. Simulated sample has a scattering coefficient of 100 cm^{-1} an anisotropic factor of 0.6 and a thickness of 0.1 cm. Starting from a dimensionless beam, and by increasing the waist value, the intensity profile at the exit of the sample broadens, although the change is not so big. However, the region at which unscattered light can be measured at the exit of the sample increases appreciatively by increasing the waist of the incident beam (indicated by the overlap region between the entrance and the exit intensity profile). For a waist of 0.20 cm,

unscattered light could be detected in a region almost as big as the region at which light exits the sample. Figure 3 shows that the optical configuration required to measure collimated transmittance depends strongly on the waist of the entrance beam, in particular pinhole size must be selected as big as the initial beam, being the later almost twice the beam waist. From now on, pinhole size was selected to be twice the initial beam waist to ensure that all non-scattered photons are detected. As will be shown below, this selection will also affect other spatial configuration for the optimal optical setups, for example minimum distance between pinholes required for a reliable measurement of the unscattered intensity.

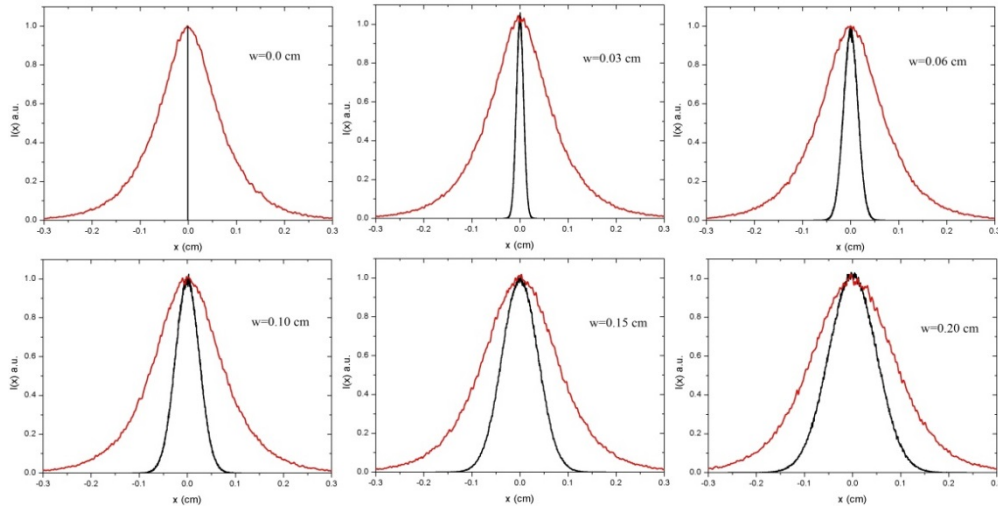


Fig. 3. Result of Monte Carlo simulation for the laser beam intensity profile at the entrance (black) and exit (red) surfaces of a turbid slab when the waist of the beam, w , is varied. Both profiles were normalized at the maximum intensity value.

In the literature, there are many optical configurations used for measuring the collimated transmittance [5–8,20], being the simplest one a configuration similar at the one shown in Fig. 2(B) in which two pinholes separated a given distance are used to selectively detect light propagating parallel to the optical axis, *i.e.* the unscattered light. Scattered light detected in a T_c measurement can be expressed as $I_{scattered}/d\Omega$, where $I_{scattered}$ is the intensity scattered by the sample and $d\Omega$ is the solid angle subtended by the detector relative to the sample, and thus has a d^{-2} dependence. The perfect configuration would require $d \rightarrow \infty$ and a perfectly collimated beam, being this experimentally hard to implement. If d is too small, contribution of scattered light from the sample to T_c measurement is bigger, thus giving an incorrect value of T_c . This incorrect measurement would affect further calculations, such as the recovery of optical properties or the measurement of the optical thickness. It is expected that the minimal distance d required to get a reliable measurement of the unscattered light depends on the optical properties of the sample. In a similar way, the diameter of the pinholes is mainly determined by the waist of the beam, as shown in Fig. 3.

Figure 4(A) presents the collimated transmittance simulated using the optical set up shown in Fig. 2(B) as a function of the distance, d , between pinholes for a sample with a scattering coefficient of 25 cm^{-1} and an anisotropic coefficient of 0.6. The beam waist used was 0.06 cm, and the diameter of the pinholes was 0.15 cm. The sample is sandwiched between two glass slides of thickness 0.15 cm and a refractive index of 1.5. The sample has a thickness, t , of 0.1 cm and a refractive index of 1.33. Figure 5 also shows the expected value of the collimated transmittance (continuous line), which in this case is 0.075 calculated as $T_c = A \exp(-\mu_s t)$ where $A = 0.917$ that corresponds to the transmittance of sample when $\mu_s = 0$. At $d = 0$, the intensity detected by the detector is higher than the expected value for the collimated

transmittance, but by increasing d , the intensity detected increases up to a distance of around 10 cm. For distances larger than 10 cm, our program correctly recovers the value of the collimated transmittance within experimental errors (continuous line). We found that the behavior of T_c vs d observed in Fig. 4(A) is a general trend for samples with larger values of the scattering coefficient, μ_s , as it is shown in Fig. 4(B). At small values of d , the intensity detected is bigger than the expected value for the unscattered light. Increasing the distance between the pinholes decreases the simulated value of T_c up to the expected theoretical value (continuous line). Note that the minimum distance required for a reliable result for the unscattered light depends on the optical properties of the sample, as expected.

Inset in Fig. 4(A) shows the minimum distance d_{min} between pinholes required to get a reliable result for the collimated transmittance as a function of the scattering coefficient μ_s . d_{min} was calculated from the distance at which the exponential fit of T_c in function of d is indistinguishable from the theoretical result, within the simulation error. It is observed from this figure that d_{min} in general increases as μ_s increases, within the explored range of distances and scattering coefficients. For the remaining of this section, the distance between pinholes was kept constant in a value of 25 cm, thus ensuring that even for the more scattering sample, the distance between pinholes is enough to give a reliable result of T_c .

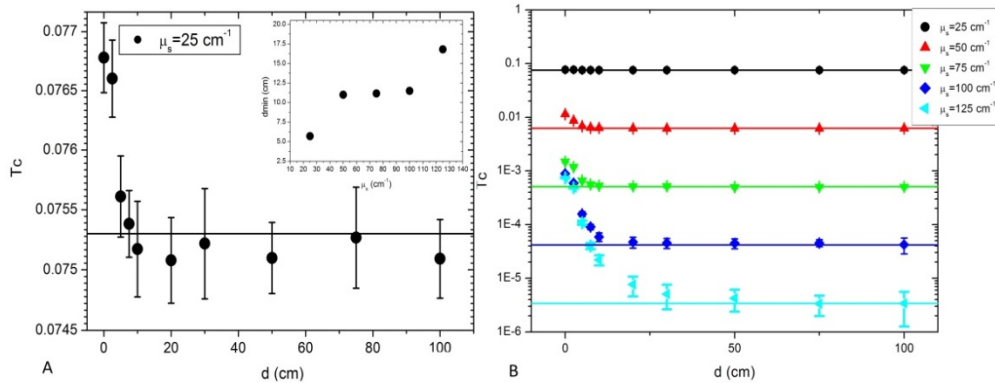


Fig. 4. A) Simulation of collimated transmittance, T_c of a sample with scattering coefficient of 25 cm^{-1} , as a function of the distance, d , between pinhole 1 and 2 for the optical set up shown in Fig. 2B. B) Result for the simulation of collimated transmittance, T_c , as a function of the distance, d , between pinhole 1 and 2 at several values of the scattering coefficient. Inset: Dependence of minimum distance between pinholes required to get a reliable result of T_c with the scattering coefficient.

For samples with $\mu_a = 0$, we expect a value for the collimated transmittance of $T_c = \exp(-\mu_s t)$, thus $\ln(T_c) = -\mu_s t$. In a log plot, the collimated transmittance should have a linear dependence with the thickness at a fixed value of μ_s , or a linear dependence with the scattering coefficient μ_s at a fixed value of t . Figure 5(A) shows the dependence of the logarithm of T_c as function of the thickness, ranging from 0 to 0.2 cm, at different values of the scattering coefficient of the sample, from $\mu_s = 10 \text{ cm}^{-1}$ up to $\mu_s = 100 \text{ cm}^{-1}$. All curves present a linear dependence with the thickness no matter the value of μ_s . Continuous lines represent the best linear fit, from which the scattering coefficient can be extracted. In a similar way, Fig. 5(B) shows the dependence of the logarithm of T_c in function of the scattering coefficient, μ_s ranging from 10 to 100 cm^{-1} , at different values of the sample thickness, from $t = 0.02 \text{ cm}$ up to $t = 0.2 \text{ cm}$. All curves show a linear dependence with the scattering coefficient, no matter the value of t . As in the previous situation, continuous lines represent the best linear fit of $\ln(T_c)$. It is easy to understand that the scattering coefficient, μ_s , can be recovered as the slope of the line that best fits the natural logarithm of simulated T_c versus the thickness, t , of the turbid slab. In a similar way, fitting this quantity to a line when the

independent variable is the scattering coefficient μ_s , will allow for retrieving the thickness, t of the slab.

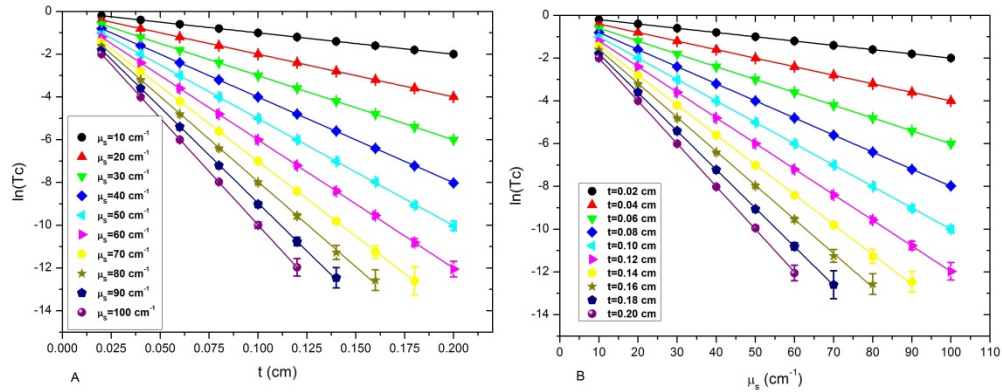


Fig. 5. Plots on the left represent a linear fit of $\ln(T_c)$ when the thickness of the slab is the independent variable while plots on the right represent a linear fit of $\ln(T_c)$ when the scattering coefficient, μ_s , of the slab is the independent variable.

A correct value of either the scattering coefficient or thickness retrieved from the procedure explained above would indicate that our program correctly calculates the collimated transmittance. Figure 6(A) shows a comparison between the scattering coefficient used in MCML simulation μ_{s-teo} and the scattering coefficient recovered from the linear fit of $\ln(T_c)$ in function of the thickness, μ_{s-sim} . Figure 6(B) shows a comparison between the thickness used in the MCML simulation t_{teo} and the thickness recovered from the linear fit of $\ln(T_c)$ in function of the scattering coefficient, t_{sim} . The continuous line with a slope of 1 would correspond to a perfect agreement. In both cases, the results obtained from the program “photon propagation program in an optical-biological system” of μ_s and t , match the values used in the MCML simulation (error bars are within the symbol size of Fig. 6). Even though simulation uncertainty is big at low values of T_c in Fig. 7, the linear fit correctly extract the optical properties or thickness of the sample, showing that our program correctly calculates the collimated transmittance up to a value on the order of 1×10^{-6} for 1,000,000 of simulated photons. Samples of a higher thickness could be simulated with our program, but a bigger amount of photons would be necessary to achieve correct results with the consequence of a noticeable cost of computational time. For a sample with a collimated transmittance on the order of 1×10^{-6} , with 25 simulations of 1,000,000 photons, around 45 minutes are required in a 4.0 GHz personal computer, giving a relative error of 30%. The use of GPU accelerated algorithms, such as GPU-MCML [21], could overcome this limitation, thus allowing the use of our hybrid algorithm to samples with larger optical thicknesses.

As pointed out previously, the collimated transmittance depends only on the optical thickness, *i.e.* on $(\mu_s + \mu_a)t$. However, the anisotropy factor g changes the spatial distribution of scattered light. Thus, a sample with a higher optical thickness scatters light mainly in the forward direction. For a weakly scattering sample with $g \rightarrow 1$, the unscattered light is more difficult to measure, because of the effect described above. To test both that the configuration chosen for our simulations is optimal and that the simulated collimated transmittance does not depend on the anisotropy factor, the collimated transmittance T_c was simulated at different values of g (0.5, 0.6, 0.7, 0.8 and 0.9) and μ_s (25, 50, 75 and 100 cm^{-1}). Figure 7(A) shows T_c in function of the anisotropy factor at different values of μ_s . In all cases, no matter the value of the scattering coefficient, our program recovers the correct value of the unscattered light within experimental error. Moreover, T_c does not present any dependence with the anisotropy factor. A sample with an anisotropy factor of 0.98, a typical value found in human tissue, was simulated, finding that the T_c recovered in the simulated situation matches the theoretical

value (data not shown), however a distance between pinholes of 75 cm was necessary; this result shows that even for highly forward scattering samples, an optimal configuration for a reliable measurement of T_c can be found using our algorithm.

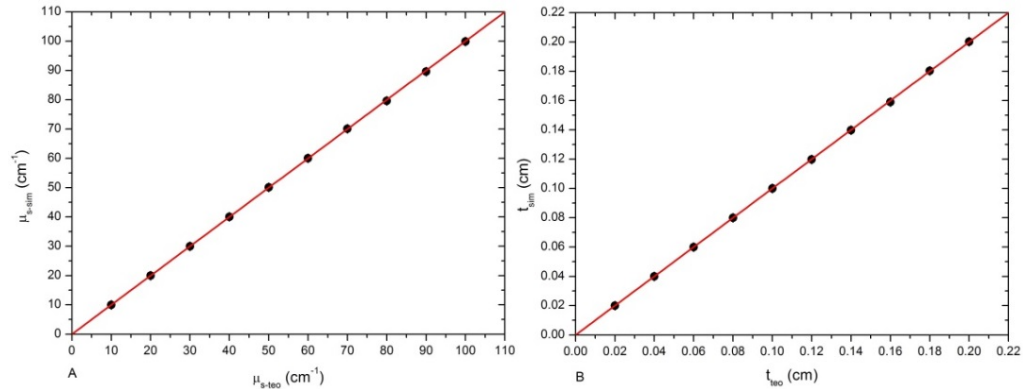


Fig. 6. a) Comparison between the scattering coefficient used in MCML simulation μ_{s-teeo} and the scattering coefficient μ_{s-sim} recovered from the linear fit of $\ln(T_c)$ as function of the thickness and b) plot of the comparison between the thickness t_{teeo} used in the MCML simulation and the thickness recovered from the linear fit of $\ln(T_c)$ as a function of the scattering coefficient.

All previous simulations were done with an absorption coefficient equal to zero. To test the validity of our algorithm in the case of a scattering and absorbing sample, we perform a simulation in an absorbing sample. The simulated sample has the following properties: $\mu_s = 50 \text{ cm}^{-1}$, $g = 0.6$, $t = 0.1 \text{ cm}$, and refractive index of 1.33. Figure 7(B) shows T_c in function of μ_a for μ_s ranging from 0 to 100 cm^{-1} . As can be seen, T_c decreases with increasing μ_a . Continuous line represents the expected value of T_c , i.e. $T_c = \exp[-(\mu_s + \mu_a)t]$. As can be seen the fit is good within experimental error. The optical properties used in the simulation are representative of a biological turbid media. Figure 7(B), altogether with the previous results shows that our algorithm simulates correctly an experimental set-up for the measurement of collimated transmittance, and can be used in a wide range of scattering properties.

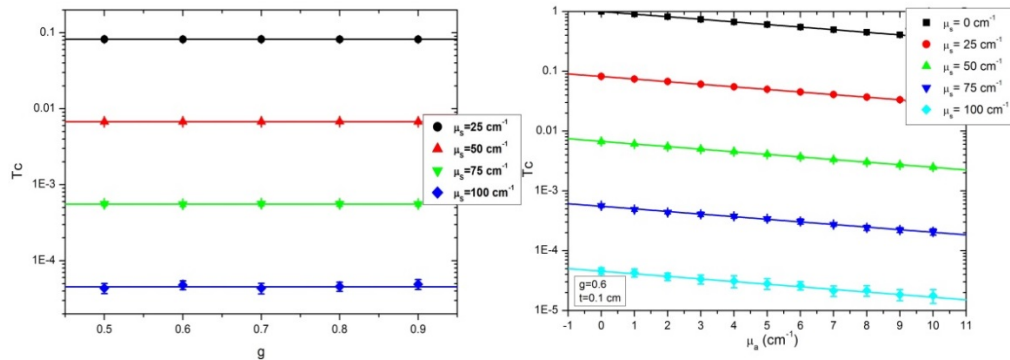


Fig. 7. A) Collimated transmittance “ T_c ” versus the anisotropy factor “ g ” at different values of μ_s when the sample is considered as a non-absorbing medium. B) Collimated transmittance “ T_c ” versus the absorption coefficient.

Finally, we used the program “photon propagation program in an optical-biological system” in a real experimental situation, namely, the measurement of the collimated transmittance of a concentrated colloidal suspension. The experimental set-up used is shown in Fig. 2, with $d = 25 \text{ cm}$. This distance was chosen using the results shown above (see Fig. 6). Figure 8 shows T_c at different values of μ_s . Experimental error bars were calculated from

optical parameters recovery and collimated transmittance experimental uncertainties. The simulation was carried out using the experimental set-up show in Fig. 2. In this case, the scattering coefficient recovered using IAD was used as an input parameter in the Monte Carlo simulation. As can be seen, both experimental and simulated collimated transmittance match the theoretical value (dashed line), calculated as $T_c = A \exp(-\mu_s t)$, where A is the transmittance of air-glass-water-glass-air interface, within experimental error.

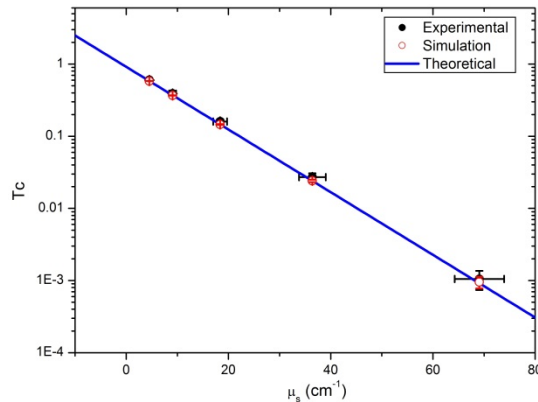


Fig. 8. Result of the comparison between the experimental dependence of “ T_c ” versus “ μ_s ” and its simulation by mean of the developed program.

Finally, is important to point out that our hybrid approach can be used for other applications related to the light distribution at the exit of a turbid media. Being based in a Monte Carlo simulation, sample geometries or spatially and directionally inhomogeneous beam sources can be easily programmed, thus opening the possibility of using our algorithm in, for example, spatial and/or angular resolved transmittance, such as goniometric measurements.

4. Conclusions

The “photon propagation program in an optical-biological system” is capable to simulate an optical system with both optical (refractive or blocking surfaces) and biological components (with scattering and absorbent properties). This program uses a modification of the MCML program to simulate light propagation within the turbid media, with an incident Gaussian profile, and the well-known refractive equations for light propagation through an optical set-up after the turbid media. We found that, for a turbid media with optical properties close to those found in biological tissue; at least one million simulated photons are required to get reliable results.

We have shown that the collimated transmittance measurement simulated with our program corresponds to those found by evaluating the Beer-Lambert law in the simplest case of no absorption. Also we found, as expected, that the collimated transmittance, *i.e.* the non-scattering light that travels parallel to the axis trough the optical set-up, is not affected by changing the anisotropic factor of the turbid media. Moreover, although all the simulations presented in this paper were performed for a homogeneous turbid media, it is important to notice that an unlimited number of layers can be used for the modeled turbid medium being this a direct consequence of the original MCML code used in our algorithm. This feature is extremely useful and advantageous, for instance, in studying the influence of optical and geometrical parameters of specific layers of a stratified media on its effective collimated transmission. The main disadvantage of our program relies in the number of photons required to get a statistically reliable result. However, a way to amend this disadvantage relies in the use of GPU-accelerated Monte Carlo Algorithms such as GPU-MCML.

Further work relies in the use of the “photon propagation program in an optical-biological system” including a Gaussian source of light for finding the optimal experimental set-up in collimated transmittance measurements of biological tissue for optical parameters recovery in biomedical applications.

Acknowledgment

The authors would like to thank Dr. Francisco Pérez Gutiérrez, Facultad de Ingeniería, Universidad Autónoma de San Luis Potosí, México, for providing us the facilities of his laboratory for the experimental part of this work.